arXiv:1611.07191v1 [cs.DS] 22 Nov 2016

Distributable Consistent Multi-Graph Matching

Nan Hu Boris Thibert Leonidas Guibas
Stanford University, Stanford, CA, USA
pkuhunan@gmail.com, boris.thibert@imag.fr, guibas@cs.stanford.edu

November 23, 2016

Abstract

In this paper we propose an optimization-based framework to multiple graph matching. The framework takes as input maps computed between pairs of graphs, and outputs maps that 1) are consistent among all pairs of graphs, and 2) preserve edge connectivity between pairs of graphs. We show how to formulate this as solving a piece-wise low-rank matrix recovery problem using a generalized message passing scheme. We also present necessary and sufficient conditions under which such global consistency is guaranteed. The key feature of our approach is that it is scalable to large datasets, while still produce maps whose quality is competent against state-of-the-art global optimization-based techniques.

1 Introduction

Graph matching techniques have been widely used in many fields of computer vision, including 2D and 3D image analysis, object recognition, biomedical identification, and object tracking. Tremendous amount of effort has been taken to find meaningful approximate isomorphism between pair of graphs [21, 6, 9, 10, 23, 8, 12, 13]. Many tasks, however, require solving the so-called multi-graph matching problem, i.e., finding consistent maps among all pairs of graphs within a collection. Examples include non-rigid structure from motion [1, 7] and shared object discovery [3]. In this context, a central task is how to utilize the data collection as a regularizer to improve the maps computed between pairs of objects in isolation [14, 4, 26].

An generic constraint that one can utilize to improve maps among a collection is the so-called *cycle consistency* constraint, namely composition of maps along any two paths sharing the same starting and end objects are identical. A technical chanllenge of utilizing this constraint is that it is impossible to check all cycles for consistency

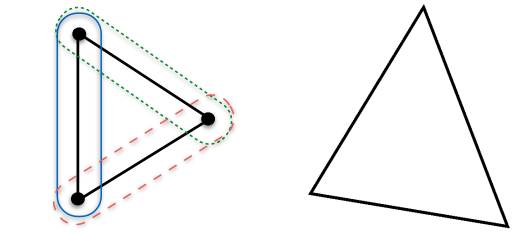

(a) Subgraphs that forms an empty triangle cover complex

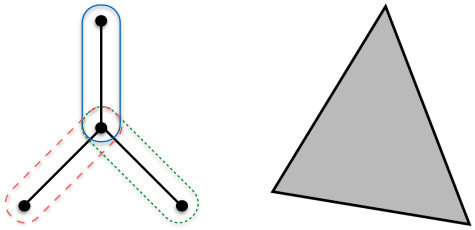

(b) Subgraphs that form an solid triangle cover complex

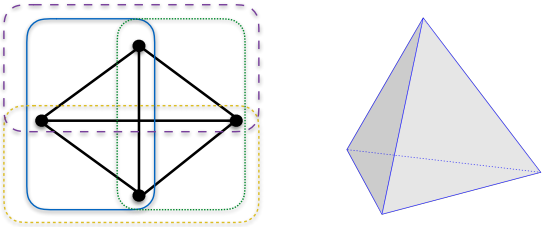

(c) Subgraphs that form an empty tetrahedron cover complex

Figure 1: Given local consistency, (a) is not globally consistent, while (b) and (c) are guaranteed to be globally consistent. (Left: the map graph with subgraphs circled out. Right: the corresponding cover complex.)

due to the fact that the number of paths increase exponentially with the total number of objects (each object is a graph in our setting). Recent works on joint matching has shown that the cycle consistency constraint can be translated into a much more manageable constraint, i.e., the data matrix that stores pair-wise maps in blocks is positive semidefinite and low-rank [19, 14]. Based on connection, people have formulated multiple-object matching as solving semidefinite programs (or SDP), which are convex relaxations of the corresponding matrix recovery problem. These algorithms achieved near-optimal exact recovery conditions [14, 4]. On the other hand, solving semidefinite programs are computationally intensive. In a recent work, Zhou et al [26] attempts to address the computational issue using alternating minimization, a fast solver for solving semidefinite programs.

In this paper, we propose a novel algorithm that utilizes the cycle-consistency constraint in a hierarchical manner for scalable multiple object matching. In particular, instead of jointly imposing the global consistency on all pair-wise maps [14, 4, 26], we split the collection of graphs into overlapping subsets, and impose consistency within each subset. We then impose consistency between maps across the subsets. Interestingly, we show that by combing these two consistency constraints together, we can guarantee global consistency under mild conditions (See Section 2). Yet computationally, such a decoupled approach yields significant performance gains, when compared with existing approaches.

1.1 Related Work

Early works on multi-graph matching are based on detecting inconsistent cycles [25, 18], and formulate multi-graph matching as solving combinatorial optimizations, i.e., removing bad maps to break all inconsistent cycles. Other people have proposed to formulate non-convex optimization problems by using the cycle consistency as an explicit constraint for either pixel-wise flow computation [26] or sparse feature matching [24]. These problems are, as a consequence, hard to solve and do not admit exact recovery conditions. Recent works [15, 14, 19] showed that consistent maps could be extracted from the spectrum of a data matrix that encodes pair-wise maps in blocks. Along this line of research, Huang and Guibas [14] proposed an elegant solution by formulating the problem as convex relaxation and discussed the theoretical conditions for exact recovery. The result is further analyzed in [4] under the condition that the underlying rank of the variable matrix is known or can be reliably estimated. These methods, however, are not scalable to large-scale datasets, due to the cost of solving semidefinite programs. Zhou et al. [26] enforce the positive semidefinite constraint using explicit low-rank factorizations, leading to improved computational efficiency. In contrast to these methods, our approach opens a new direction to enforce the cycle-consistency constraint, i.e., by splitting the datasets into overlapping subsets. This leads to further improvements in terms of computational efficiency.

We organize the reminder of this paper as follows. Firstly, we discuss the problem setup and analyze the conditions In Section 2. Secondly, we discuss the formulation of our approach In Section 3. In the following Section 4, we present an alternating direction method of multipliers (ADMM) for solving the induced optimization problem, leading to a parallel algorithm via generalized message passing. Last but not the least, we demonstrate the effectiveness of our approach on both synthetic and real examples in Section 5.

2 Consistency

In this section, we define consistency in graph matching and discuss conditions under which the graph matching results are guaranteed to be consistent.

Firstly, we will introduce some notations and definitions that will be used to demonstrate our work throughout the paper. In multi-graph matching, we consider two levels of graphs, i) *the matching graphs* and ii) *the map graph*. *The matching graphs* represent the collection of graphs that we intend to find matches in, i.e. to find vertex level correspondences among them. Let G_i denote a matching graph[1] and $\mathcal{V} = \{G_i\}$ be the set of matching graphs. While *the map graph* represents another level of abstraction, where each vertex encode a matching graph, and the edges encode their base maps. A base map from G_i to G_j is denoted by $\phi_{ji} : G_i \mapsto G_j$[2] and could be thought of as the initial noisy matchings between G_i and G_j[3]. Finally , let $\mathcal{G} = \{\mathcal{V}, \mathcal{E}\}$ denote the map graph, where an edge $e_{ij} \in \mathcal{E}$ whenever ϕ_{ij} exists.

Suppose $G_i - G_j - G_k$ is a path in $\mathcal{G}$, let $\phi_{kj} \circ \phi_{ji}$ denote the composite map along this path.

Definition 1 (Cycle Consistency)**.** *A map graph $\mathcal{G} = \{\mathcal{V}, \mathcal{E}\}$ is* cycle consistent *if for every node G_i and every cycle $G_i - G_j - \cdots - G_k - G_i$, the composite map*

[1] One example is as in Section 5 on image keypoint matching. In G_i, vertices encode the keypoints and edges encode the application-dependent inter-keypoints relationship from an image.

[2] We assume the maps are invertible, i.e. $\phi_{ij} = \phi_{ji}^{-1}$.

[3] This initial matching, namely the base map, could come from any of the existing pairwise matching algorithms, e.g. [5, 12, 13].

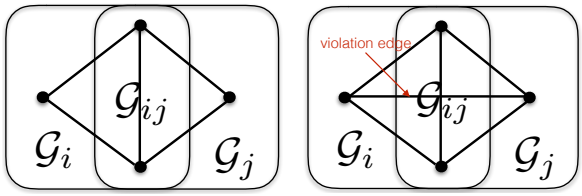

(a) *joint normal* (b) Counter *joint normal*

Figure 2: Examples of subgraphs that are (a) joint normal and (b) not joint normal.

along the cycle is the identity map, i.e.

$$\phi_{ik} \circ \cdots \circ \phi_{ji} = \text{identity}$$

Definition 2 (Joint Normal)**.** *Let $\mathcal{G}_i = \{\mathcal{V}_i, \mathcal{E}_i\}$, $\mathcal{G}_j = \{\mathcal{V}_j, \mathcal{E}_j\}$ be the two subgraphs of $\mathcal{G}$ and let $\mathcal{G}_{ij}$ be the intersection subgraph, i.e. the subgraph induced by $\mathcal{V}_i \cap \mathcal{V}_j$. Then we call $\mathcal{G}_i$ and $\mathcal{G}_j$* joint normal *if $\mathcal{G}_{ij}$ is connected and*

$$e_{ij} \notin \mathcal{E},\ \forall G_i \in \mathcal{V}_i \backslash \mathcal{V}_j, G_j \in \mathcal{V}_j \backslash \mathcal{V}_i$$

Literally, that two subgraphs are *joint normal* means their intersection subgraph is either empty or connected and there is no edge between a vertex in one subgraph to a vertex in the other except possibly those in their intersection subgraph, as illustrated in Fig. 2. The case in Fig. 2 (b) is not *joint normal* because such an edge exists and hence violates the condition.

Definition 3 (Cover Complex)**.** *Let the collection of sets of graphs $\mathcal{V}_\mathcal{G} = \{\mathcal{V}_i\}$ be a cover of $\mathcal{G}$, i.e. $\cup_i \mathcal{V}_i = \mathcal{V}$. Under the regular operation of set intersection, we build a simplicial complex $\mathcal{K}$, where for every subset $\{\mathcal{V}_{i_1}, \cdots, \mathcal{V}_{i_k}\}$ of $\mathcal{V}_\mathcal{G}$, we have a simplex $\sigma \in \mathcal{K}$ of dimentionality $k-1$ taking $\mathcal{V}_{i_1}, \cdots, \mathcal{V}_{i_k}$ as vertices if the subset has none empty intersection, i.e. $\cap_j \mathcal{V}_{i_j} \neq \varnothing$. We call $\mathcal{K}$ the cover complex of $\mathcal{V}_\mathcal{G}$.*

We can now state the cycle consistent matching theorem that relates global and local cycle consistency. Intuitively, this theorem states that if the cover complex $\mathcal{K}$ is connected, then the global consistency is obtained from the local cycle consistency for each subgraph $\mathcal{G}_i$ and from the compatibility condition that every two intersecting subgraphs $\mathcal{G}_i$ and $\mathcal{G}_j$ are *joint normal*.

Theorem 1 (Cycle Consistent Matching)**.** *Let $\mathcal{G}$ be a map graph, $\mathcal{V}_\mathcal{G}$ be a cover of $\mathcal{G}$, and $\mathcal{K}$ be the cover complex of $\mathcal{V}_\mathcal{G}$. Let $\mathcal{G}_i = \{\mathcal{V}_i, \mathcal{E}_i\}$ be the subgraph of $\mathcal{G}$ induced by $\mathcal{V}_i$. Then, a matching on $\mathcal{G}$ is cycle consistent iff*

1. *$\mathcal{G}_i$ is* cycle consistent *$\forall i$,*
2. *$\mathcal{G}_i$ and $\mathcal{G}_j$ are* joint normal *$\forall i, j$,*
3. *$\mathcal{K}$ is* simply connected*.*

The proof to Theorem 1 is left to Appendix A. Note, the 3nd condition in Theorem 1 is necessary. A simple counter example would be as shown in Figure 1(a). For any given pairwise mappings, they apparently satisfy 1st and 2nd conditions in Theorem 1. The cover complex $\mathcal{K}$, however, is homologous to the Torus, T^2 and thus have a non-trivial cycle, which violates condition (3). It is easy to show that there would be no global cycle consistency.

On the other hand, a counter-intuitive example is as in Figure 1(c), where $\mathcal{K}$ is a tetrahedron without interior, and is homologous to the Sphere, S^2. Although this $\mathcal{K}$ also has an empty interior, it actually satisfies our condition (3) and hence it gives global consistency. Interested readers could verify the results themselves.

As a consequence, Theorem 1 gives a practical guidance on the construction of a cover. Think of special cases when $\mathcal{K}$ is simply connected. One case is when $\mathcal{K}$ is homologous to a disc, B^1. Suppose $\mathcal{G}$ has a geometrical realization, and this could be done with any of the existing graph embedding algorithms, either globally or locally. We could then build a α-complex on top of the embedding, and it's know that when the radius r is large enough, the topology of the α-complex is guaranteed to be homologous to B^1, and therefore simply connected. Another case is when $\mathcal{K}$ is tree-structured[4]. This could be done by finding the maximum spanning tree of a given $\mathcal{K}$. Finding the best cover is an interesting topic per se. It is, however, outside the scope of the paper.

3 Distributed Optimization

3.1 Formulation

Given a map graph $\mathcal{G}$ and a cover $\mathcal{V}_\mathcal{G}$, we formulate the distributed *cycle consistency* problem from the observation in Theorem 1. Following the state-of-the-art work on convex relaxation of maps [4, 26], we encode the base map ϕ_{ji} into matrix form as $\overline{\mathbf{X}}_{ij} \in \{0,1\}^{|G_i| \times |G_j|}$ where $\overline{\mathbf{X}}_{ij}(s, s') = 1$ iff $(s, s') \in \phi_{ji}$. Let $\overline{\mathbf{X}}_\mathcal{V}$ be the matrix form of matching for vertices set $\mathcal{V}$, i.e.

$$\overline{\mathbf{X}}_\mathcal{V} = \begin{pmatrix} \mathbf{I} & \overline{\mathbf{X}}_{12} & \cdots & \overline{\mathbf{X}}_{ij} \\ \overline{\mathbf{X}}_{21} & \mathbf{I} & \cdots & \vdots \\ \vdots & \cdots & \ddots & \vdots \\ \overline{\mathbf{X}}_{ji} & \cdots & \cdots & \mathbf{I} \end{pmatrix}$$

[4] In our experiment, we constructed tree-structured cover complex $\mathcal{K}$ from Fiedler vector of the map quality graph, where we associate each edge in the map graph $\mathcal{G}$ a quality score.

Let n be the number of matching graphs, m_i be the number of vertices in matching graph G_i. $\overline{\mathbf{X}}_{\mathcal{V}}$ represents the noisy input in our formulation. Let $\mathbf{X}_{\mathcal{V}}$ be the optimization variable which encodes the desired cycle consistency property. Assuming there's a hidden universal identity space, we know that $\mathbf{X}_{\mathcal{V}}$ should be intrinsically low rank and positive semidefinite[5], i.e. there exists a mapping matrix $\mathbf{A}_{\mathcal{V}}$, such that $\mathbf{X}_{\mathcal{V}} = \mathbf{A}_{\mathcal{V}}\mathbf{A}_{\mathcal{V}}^\top$. Similar to [4, 26], we add necessary additional constraints and relax the integer constraint. Our $h(\mathcal{V})$ is formulated as

$$\begin{array}{ll} \min & \langle \mathbf{W}_{\mathcal{V}}, \mathbf{X}_{\mathcal{V}} \rangle + \lambda \|\mathbf{X}_{\mathcal{V}}\|_* \\ \text{s.t.} & \mathbf{X}_{\mathcal{V}} \succeq 0, \\ & \mathbf{X}_{\mathcal{V}(ii)} = \mathbf{I}_{m_i}, \forall i \\ & \mathbf{X}_{\mathcal{V}(ij)} = \mathbf{X}_{\mathcal{V}(ji)}^\top, \forall i \neq j \\ & 0 \leq \mathbf{X} \leq 1 \end{array} \tag{1}$$

where $\langle \cdot, \cdot \rangle$ is the matrix inner product, $\|\cdot\|_*$ is the matrix nuclear norm, and $\mathbf{W}_{\mathcal{V}} = \alpha \mathbf{1} - \overline{\mathbf{X}}_{\mathcal{V}}$[6]. The purpose of adding constant α is to impose L_1 constraint on $\mathbf{X}_{\mathcal{V}}$ for sparsity. We use $\mathbf{X}_{\mathcal{V}(ij)}$ to denote the $(i,j)^{\text{th}}$ block of the block matrix $\mathbf{X}_{\mathcal{V}}$. As has been shown in [26], the constraint $\mathbf{X}_{\mathcal{V}} \succeq 0$ could be relaxed if λ is big enough. Let $\mathcal{C}_i$ encodes the convex set induced by the rest of the constraints for $\mathcal{V}_i$, we could then simplify the notation of our optimization problem for $h(\mathcal{V}_i)$ to be

$$\begin{array}{ll} \min & \langle \mathbf{W}_{\mathcal{V}_i}, \mathbf{X}_{\mathcal{V}_i} \rangle + \lambda \|\mathbf{X}_{\mathcal{V}_i}\|_* \\ \text{s.t.} & \mathbf{X}_{\mathcal{V}_i} \in \mathcal{C}_i \end{array}$$

Let $\mathbf{X}_{\mathcal{V}_{i\cap j}^i}$ be the mapping matrix of $\mathcal{V}_{i\cap j}$ in $\mathcal{V}_i$, i.e. a submatrix of $\mathbf{X}_{\mathcal{V}_i}$ by picking blocks that belongs to the matching graphs in $\mathcal{V}_{i\cap j}$. From Theorem 1, we could then formulate our distributed problem as

$$\begin{array}{ll} \min & \sum_i \left(\langle \mathbf{W}_{\mathcal{V}_i}, \mathbf{X}_{\mathcal{V}_i} \rangle + \lambda \|\mathbf{X}_{\mathcal{V}_i}\|_* \right) \\ \text{s.t.} & \mathbf{X}_{\mathcal{V}_i} \in \mathcal{C}_i \\ & \mathbf{X}_{\mathcal{V}_{i\cap j}^i} = \mathbf{X}_{\mathcal{V}_{i\cap j}^j}, \forall (i,j) \in \mathcal{E} \end{array} \tag{2}$$

3.2 Relation to global optimization

Consider the objective function as in (1) and in (2), irrespective of the nuclear norm regularization term, and let d_i, d_{ij} be the degree of replica for a matching graph G_i and an edge e_{ij} in $\mathcal{V}_{\mathcal{G}}$ respectively[7]. Let $\mathbf{d}$ be the vector form of d_i's and d_{ij}'s, we could then have

$$\sum_i \langle \mathbf{W}_{\mathcal{V}_i}, \mathbf{X}_{\mathcal{V}_i} \rangle = \langle \mathbf{W}_{\mathcal{V}}(\mathbf{d}), \mathbf{X}_{\mathcal{V}} \rangle$$

where $\mathbf{W}_{\mathcal{V}}(\mathbf{d})$ is defined as

$$\mathbf{W}_{\mathcal{V}}(\mathbf{d})_{ij} = \begin{cases} d_{ij}(\alpha \mathbf{1} - \overline{\mathbf{X}}_{ij}), & i \neq j \\ d_i(\alpha \mathbf{1} - \mathbf{I}), & i = j \end{cases}$$

This is equivalent to say that the objective in distributed formulation as in (2) is a re-weighted objective in (1). The weights are proportional to the degree of a matching graph in the cover $\mathcal{V}_{\mathcal{G}}$. This is also reasonable because in general the matching graphs connecting multiple cover nodes are more representative and hence should be more reliable.

4 Alternating minimization

4.1 Algorithms

The nuclear norm minimization in (2) can be efficiently optimized thanks to recent results on low-rank optimization by a change of variables $\mathbf{X}_{\mathcal{V}_i} = \mathbf{A}_{\mathcal{V}_i}\mathbf{B}_{\mathcal{V}_i}^\top$ as in [2, 11, 26], together with the guarantee in [20] for nuclear norm

$$\|\mathbf{X}\|_* = \min_{\mathbf{A},\mathbf{B}:\mathbf{A}\mathbf{B}^\top = \mathbf{X}} \frac{1}{2} \left(\|\mathbf{A}\|_F^2 + \|\mathbf{B}\|_F^2 \right).$$

Let $\mathbf{X}_{\mathcal{V}_i}$ and $\mathbf{X}_{\mathcal{V}_{i\cap j}}^i$ be shortened as $\mathbf{X}_i$ and $\mathbf{X}_{ij}$ respectively, the optimization problem in (2) could be rewritten as

$$\begin{array}{ll} \min & \sum_i \left(\langle \mathbf{W}_i, \mathbf{X}_i \rangle + \frac{\lambda}{2} \|\mathbf{A}_i\|_F^2 + \frac{\lambda}{2} \|\mathbf{B}_i\|_F^2 \right) \\ \text{s.t.} & \mathbf{X}_i = \mathbf{A}_i \mathbf{B}_i^\top \\ & \mathbf{X}_{ij} = \mathbf{X}_{ji}, \forall (i,j) \in \mathcal{E} \end{array} \tag{3}$$

where we omit the constraints that $\mathbf{X}_i$ and $\mathbf{X}_{ij}$ has to be in a convex set respectively.

Moreover, let $\mathbf{E}_{ij}$ denote the selection matrix to extract the part of $\mathbf{X}_i$ that belongs to the set of $\mathcal{V}_i \cap \mathcal{V}_j$, i.e.

$$\mathbf{E}_{ij} = \begin{bmatrix} \mathbf{e}_{i1} & \mathbf{e}_{i2} & \cdots & \mathbf{e}_{i|\mathcal{V}_i \cap \mathcal{V}_j|} \end{bmatrix},$$

where

$$\mathbf{e}_{ik} = \begin{bmatrix} 0 & \cdots & 0 & \underbrace{\mathbf{I}}_{s\text{-th block}} & 0 & \cdots & 0 \end{bmatrix}^\top.$$

assuming we select s-th block out of $\mathbf{X}_i$ as the k-th block in $\mathbf{X}_{ij}$. We could then rewrite $\mathbf{X}_{ij} = \mathbf{E}_{ij}^\top \mathbf{X}_i \mathbf{E}_{ij}$. As a consequence, the condition on consistent mapping within the intersections, $\mathbf{X}_{ij} = \mathbf{X}_{ji}$, becomes $\mathbf{E}_{ij}^\top \mathbf{X}_i \mathbf{E}_{ij} = \mathbf{E}_{ji}^\top \mathbf{X}_j \mathbf{E}_{ji}$. In this way, we could remove the optimization variables $\mathbf{X}_{ij}$ in (3) to have only $\mathbf{X}_i$'s and deal with the intersection consistency constraints implicitly.

[5] Minimizing the matrix rank is non-convex. A general relaxation approach is to instead minimize the nuclear norm as is shown in (1).

[6] $\mathbf{1}$ denote the matrix of all 1's.

[7] It is the total of number of cover nodes that include G_i and e_{ij} respectively, i.e. $d_i = \sum_k I(G_i \in \mathcal{V}_k)$, $d_{ij} = \sum_k I(G_i \in \mathcal{V}_k, G_j \in \mathcal{V}_k)$, where $I(\cdot)$ is the indicator function.

We then finalize our formation of the problem in (2) as

$$\begin{array}{ll}\min & \sum_i \left(\langle \mathbf{W}_i, \mathbf{X}_i\rangle + \frac{\lambda}{2}\|\mathbf{A}_i\|_F^2 + \frac{\lambda}{2}\|\mathbf{B}_i\|_F^2\right) \\ \text{s.t.} & \mathbf{X}_i = \mathbf{A}_i\mathbf{B}_i^\top, \\ & \mathbf{E}_{ij}^\top \mathbf{X}_i \mathbf{E}_{ij} = \mathbf{E}_{ji}^\top \mathbf{X}_j \mathbf{E}_{ji}, \\ & \mathbf{X}_i \in \mathcal{C}_i, \end{array} \tag{4}$$

We apply ADMM to (6), and the augmented Lagrangian is

$$\begin{aligned}\mathcal{L} = \sum_i \Bigg(& \langle \mathbf{W}_i, \mathbf{X}_i\rangle + \frac{\lambda}{2}\|\mathbf{A}_i\|_F^2 + \frac{\lambda}{2}\|\mathbf{B}_i\|_F^2 \\ & + \langle \mathbf{Y}_i, \mathbf{X}_i - \mathbf{A}_i\mathbf{B}_i^\top\rangle + \frac{\mu}{2}\|\mathbf{X}_i - \mathbf{A}_i\mathbf{B}_i^\top\|_F^2\Bigg) \\ & + \sum_{i,j}\Big(\langle \mathbf{Z}_{ij}, \mathbf{E}_{ij}^\top\mathbf{X}_i\mathbf{E}_{ij} - \mathbf{E}_{ji}^\top\mathbf{X}_j\mathbf{E}_{ji}\rangle \\ & + \frac{\beta}{2}\|\mathbf{E}_{ij}^\top\mathbf{X}_i\mathbf{E}_{ij} - \mathbf{E}_{ji}^\top\mathbf{X}_j\mathbf{E}_{ji}\|_F^2\Big)\end{aligned} \tag{5}$$

The constraints on $\mathbf{X}$'s in convex set are handled implicitly and updated in the alternating algorithm. Here, $\mathbf{Y}_i$'s and $\mathbf{Z}_{ij}$'s, are dual variables. The ADMM algorithm therefore updates primal variables by minimizing $\mathcal{L}$ and dual variables by gradient descent.

Algorithm 1: Distributed Graph Matching via ADMM

Input : Pairwise basemaps $\overline{\mathbf{X}}_i$
Output: Consistent matches $\mathbf{X}_i$

Initialize $\mathbf{A}_i$, $\mathbf{B}_i$ randomly, and set $\mathbf{Y}_i$, $\mathbf{Z}_{ij}$ to be $\mathbf{0}$
$\mathbf{W}_i = \alpha\mathbf{1} - \overline{\mathbf{X}}_i$
while *not converged* **do**
  /* inner-node update */
  $\mathbf{A}_i \leftarrow (\mathbf{X}_i + \frac{1}{\mu}\mathbf{Y}_i)\mathbf{B}_i(\mathbf{B}_i^\top\mathbf{B}_i + \frac{\lambda}{\mu}\mathbf{I})^\dagger$
  $\mathbf{B}_i \leftarrow (\mathbf{X}_i + \frac{1}{\mu}\mathbf{Y}_i)\mathbf{A}_i(\mathbf{A}_i^\top\mathbf{A}_i + \frac{\lambda}{\mu}\mathbf{I})^\dagger$
  $\mathbf{X}_i \leftarrow \mathcal{P}_{\mathcal{C}_i}(\mathbf{X}_{i0})$
  $\mathbf{Y}_i \leftarrow \mathbf{Y}_i^k + \mu\left(\mathbf{X}_i - \mathbf{A}_i\mathbf{B}_i^\top\right)$
  $\mathbf{Z}_{ij} \leftarrow \mathbf{Z}_{ij}^k + \beta\left(\mathbf{M}_{i\to j}^{k+1} - \mathbf{M}_{j\to i}^{k+1}\right)$
  /* inter-node information exchange */
  node j send $\mathbf{M}_{j\to i} = \mathbf{E}_{ji}^\top\mathbf{X}_j\mathbf{E}_{ji}$ to node i
end
Quantize $\mathbf{X}_i$ with a threshold of 0.5.

The ADMM solver for (7) is summarized in Algorithm 1 (c.f. Appendix B for details). $\mathbf{A}_i$ and $\mathbf{B}_i$ have a least square style close-form update, and $\mathbf{X}_{i0}$ is the solution to the linear equation

$$\begin{aligned}\mu\mathbf{X}_i + 2\beta\sum_j \mathbf{E}_{ij}\mathbf{E}_{ij}^\top\mathbf{X}_i\mathbf{E}_{ij}\mathbf{E}_{ij}^\top = \mu\mathbf{A}_i\mathbf{B}_i^\top - (\mathbf{W}_i + \mathbf{Y}_i) \\ + \sum_j \mathbf{E}_{ij}(2\beta\mathbf{M}_{j\to i}^k - \mathbf{Z}_{ij} + \mathbf{Z}_{ji})\mathbf{E}_{ij}^\top\end{aligned}$$

Furthermore, the update on $\mathbf{X}_i$ requires a projection onto the convex set $\mathcal{C}$, $\mathcal{P}_{\mathcal{C}}(\cdot)$, i.e. $\mathcal{P}_{\mathcal{C}}(\mathbf{X}_0)$ is the solution to the problem

$$\min_{\mathbf{X}\in\mathcal{C}} \|\mathbf{X} - \mathbf{X}_0\|_F^2.$$

This is essentially a linear programming problem, and can be solved efficiently.

4.2 Complexity

The computational complexity of Algorithm 1 is dominated by the matrix multiplication. In our proposed algorithm, the complexity per iteration is controlled by the leading node in $\mathcal{G}$, i.e. $O\left(\max_i(m_i)^2\max_i(k_i)\right)$, where m_i is the total number of points in all graphs in $\mathcal{V}_i$. This is in comparison with the state-of-the-art algorithm on consistent graph matching as in [4, 26], where the complexity per iteration is $O((\sum_i m_i)^3)$ and $O((\sum_i m_i)^2 k)$ respectively. Furthermore, in our experiment, we found the total number of iterations to converge for our algorithm is comparable as with the global method in [26].

5 Experiments

5.1 Simulation

We follow the state-of-the-art work using the same parameter setting in synthesized data evaluation as in [4, 26]. Given an optimized matching matrix $\mathbf{X}^*$ and the ground truth mapping $\mathbf{X}_g$, the error rate is measured by intersection over union:

$$1 - \frac{|\tau(\mathbf{X}^*) \cap \tau(\mathbf{X}_g)|}{|\tau(\mathbf{X}^*) \cup \tau(\mathbf{X}_g)|}$$

where $\tau(\cdot)$ denote the mapping from the matching matrix and $|\cdot|$ denote the cardinality of the set. Note in our distributed setting, we could only partially recover $\mathbf{X}^*$ given $\mathbf{X}_i^*$'s. Therefore, our ground truth setting is also different from [4, 26] by incorporating this fact.

5.1.1 Matching Errors

We evaluation our algorithm, hereafter we call it DMatch, by a comparison with MatchALS from [26]. The total

number of graphs is denoted by n. The size of the universe is set to a fixed $r = 20$ points and in each graph, a point is randomly observed with a probability ρ_0. We simulate error corruption by randomly removing true mapping and adding false ones to achieve an corruption rate ρ_e.

In experiment, firstly, we construct our cover graph by making a sparse three way tree. This was done by randomly select a subset as a common intersection $\mathcal{V}_c$ and split the rest into the three cover nodes $\mathcal{V}'_1, \mathcal{V}'_2, \mathcal{V}'_3$. As a consequence, each cover node is equal to $\mathcal{V}_i = \mathcal{V}_c \cup \mathcal{V}'_i$. In a second setup, we increase the overlap density by circularly adding one split to each cover, i.e. $\mathcal{V}_i = \mathcal{V}_c \cup \mathcal{V}'_i \cup \mathcal{V}'_{i+1}$.

In varying the parameters ρ_0, ρ_e, and n, we could then perform a comparison of DMatch with MatchALS. In both algorithms, we set $k = 2r$, and $\lambda = 50$.

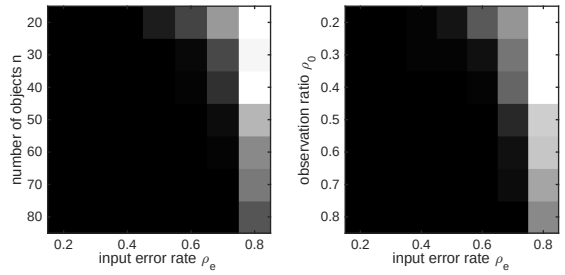

(a) DMatch-sparse

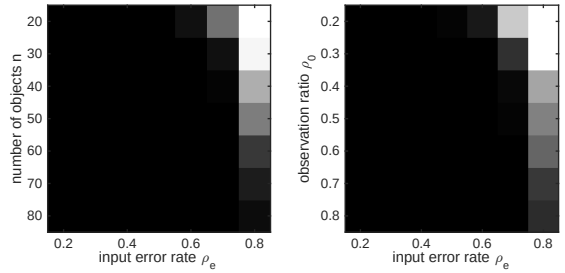

(b) DMatch-dense

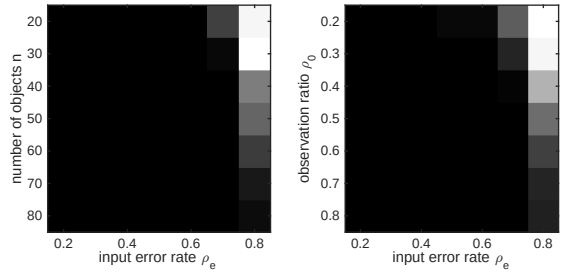

(c) MatchALS

Figure 3: Matching error comparison. Darker color means lower matching error. The fixed parameter is set to $\rho_0 = 0.6$ and $n = 50$ respectively.

Figure 3 shows matching errors under various configurations, for both DMatch and MatchALS. In general, lowering input error and increasing observation ratio or increasing the total number of objects will improve the matching performance, i.e. with a lower matching error. In addition, we could see that increasing the overlap between cover nodes would have a positive impact on the recovery (comparison between Figure 3(a) and Figure 3(b)).

Futhremore, in a comparison between Figure 3(b) and Figure 3(c), it could be seen that when the cover are dense enough, i.e. the size of the overlaps are sufficiently large, the matching error would approach that from MatchALS, which is the global recovery.

5.1.2 Graph Covers

In a second experiment, we are aimed to understand more on the effect of graph covers. In comparison, we construct a ground truth graph cover by selecting a sparse cover as in Section 5.1.1. for every pair of graphs within the same cover node, we set the error rate to be ρ_{in} and for every pair between different cover node, we set the error rate to be ρ_{out}. The experiment is then conducted by a comparison of 1) using the ground truth cover and 2) using a randomly constructed cover.

The experimentation results are shown in Figure 4. In Figure 4(a), we could see that using ground truth cover, the matching performance does not depend much on ρ_{out} as we are not using any information provided there anyway. While on randomly constructed cover, the two error rates are mixed together, and the results favor more on small ρ_{in} and small ρ_{out} at the same time. This situation, however, is changed when the cover becomes denser. The dependency on ρ_{out} disappears as shown in Figure 4(b). One reason we could think of is because the portion of out-node pairs become smaller with denser cover. As a consequence, the mixed error rate is dominated by ρ_{in}. In addition, we could also see that with denser cover, the algorithm is more error tolerant. This comes with a trade-off that on average the size of each cover becomes bigger and the computational cost also increases.

5.2 Real Experiments

5.2.1 CMU House Sequence

In this part of the experiment, we want to simulate and test the scalability of our distributed algorithm. We use the CMU House sequence [8] as the testing images. This sequence has been widely used to test different graph match-

[8] http://vasc.ri.cmu.edu//idb/html/motion/house/index.html

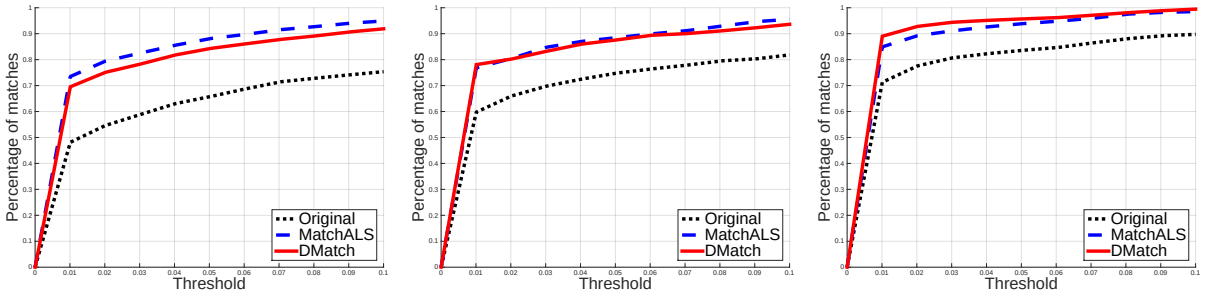

(a) Graffiti (b) Bikes (c) Leuven

Figure 5: Error curve on Graffit, Bikes and Leuven datasets. The y-axis is the correct match ration and the x-axis is the threshold value over the image width. We only compare with MatchALS (blue dahed) and original pariwise matching (black dotted) with DMatch (red solid). For more comparison with other state-of-the-art algorithms, please refer to [26].

ing algorithms. It consists of 110 frames, and there are 30 feature points labeled consistently across all frames. We use the geometry based constraint in pairwise matching as is done in [13]. To construct a valid cover complex $\mathcal{K}$, firstly we build a matching quality graph using the output pairwise matching score as the weight. Because the Fielder vector of the graph describes the connectivity of it, we split the range of the Fielder vector into 5 overlapping intervals where we try to balance the number of images contained within each interval. In this way, we build a line-structured cover complex with 5 cover nodes, and the max number of images contained in all the covers are 45. We run our DMatch algorithm comparing with the global MatchALS algorithm. The algorithm is implemented in a single laptop, we measure the time used in each cover node separately and then take the max as the total computational time per iteration, where we assume the cost for messages passed between adjacent cover nodes are negligible.

Table 1 shows the matching accuracy, timing and iterations used in these algorithms. DMatch used less iterations to converge, and achieved a total speed-up of over 6X compared with MatchALS, while maintaining an error rate of 0. One reason for this could be the graph cover structure grouped together images that have high pairwise matching quality and explicitly disregard any pairwise matchings that are of low quality (covers are joint normal), and as a consequence, it converges using less iterations. MatchALS however has to deal with low quality matches in a global sense, which seems have had negative effects on the solution, and therefore they have a relatively higher error rate.

	Original	MatchALS	DMatch
Error Rate	0.1445	0.1034	**0**
Total Iterations	-	267	**179**
Time	-	195.1	**31.7**

Table 1: The error rate, and the total computation time (seconds) on CMU House sequence.

5.2.2 Graffiti datasets

In this part of experimentation, we follow the procedure as described in [26]. We use the benchmark datasets from Graffiti datasets [9]. In each dataset there are 6 images of a scene with various image transformations, including viewpoint change, blurring, and illumination variation etc.

To construct an affinity score matrix $\overline{\mathbf{X}}$, we employ the same procedure as in [26] for comparison purpose. We first detect 1000 affine covariant feature [17] points in each image of the dataset and compute their SIFT [16] descriptors using VLFeat library [22]. The affinity scores are computed as the inner product between every pair of detected feature points on each pair of images. We exclude apparent mismatches be keeping only affinity scores that are above the threshold 0.7. Furthermore, any potential matches that are indistinguishable is removed, i.e. if the first and the second top matches are below the ratio threshold 1.1, the candidate point is removed. Finally, any feature point that has only one candidate match in the dataset is also excluded.

In a comparison, to construct our cover graph, we first build a matching quality graph, using the matching score as the edge weight and use the Fiedler vector of the graph

[9] http://www.robots.ox.ac.uk/~vgg/data/data-aff.html

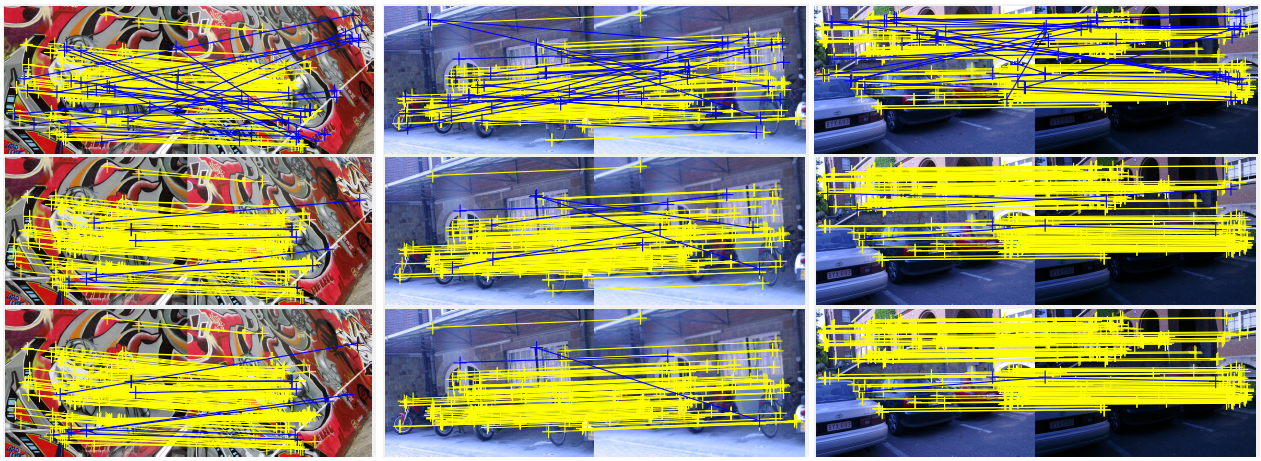

(a) Graffiti (b) Bikes (c) Leuven

Figure 6: Example of matching results. The bottom one is from DMatch, the middle is from MatchALS and the top one is from original pairwise matching respectively. Yellow lines encode the correct matches, while blue lines are for wrong ones.

laplacian to split the images. In order to have an overlap between the two cover nodes, we include a buffer at the clustering boundary to have one image on the positive side fuse into the negative cluster and vice versa. This way each cover node contains 4 images and the overlap between them has two images.

To evaluate the performance, we use the ground truth homography matrix given in the dataset, and adopt the procedure used in [4]. For a test point, we calculate the true correspondence using homography and compare with the matched correspondence. If they are within a predefined distance threshold, we deem the matching is correct, and otherwise, wrong. Then we sweep along the threshold dimension to draw an error curve that is dependent on the threshold chosen. Figure 5 showed the curve for three datasets, Graffiti, Bikes, and Leuven. To have a fair comparison, and note that our DMatch will not give a full pairwise matching between images, instead, we only have a matching when the two images belong to the same cover node. Therefore, we compute the one-hop composite match between image pairs across different cover nodes[10].

In Figure 6, we show the example matches between the first and the fourth image for each dataset. The bottom match is DMatch, the middle is MatchALS and the top one is the original pairwise map. Clearly, our matching shows almost exactly the same results as MatchALS, where both corrected mismatches (reduced blue lines) and increased correct matches (denser yellow lines).

In our implementation [11], we notice that the total number of iterations to converge for both DMatch and MatchALS are roughly the same (around 60 iterations).

6 Conclusion

In this paper, we provided a framework to jointly match multiple graphs in a consistent manner that is completely scalable and distributable. We designed an algorithm aiming for local and global consistency at the same time by information exchange per iteration. Furthermore, we theoretically proved the necessary and sufficient conditions under which locally consistent matchings would guarantee global consistency. In our experiments, we showed that the joint matching could be done in a distributed way without sacrificing performance. We believe this is a very important first step for large scale exploration of images for object matching as well as building 3D object models from crowdsourced collections. Future work includes matching large collection of different objects that have high similarity and enough variance, e.g. a collection of different dogs or cats.

[10] For each image i and j not in the same cover node, we loop through all $k \neq i, j$ and accumulate the composite matchings from $i \to k$ and $k \to j$.

[11] Thanks for the authors of [26] to kindly provide their original implementation of the algorithm.

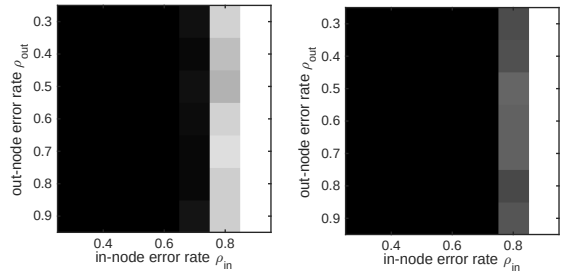

sparse dense

(a) ground truth cover

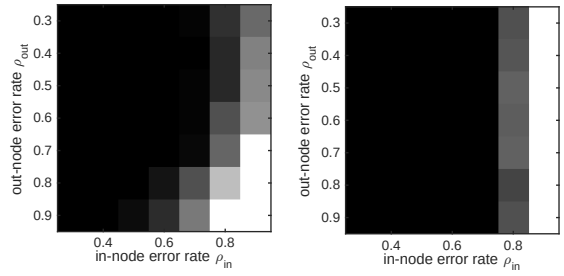

sparse dense

(b) randomly constructed cover

Figure 4: Effects on recovery from the construction of graph cover. Darker color means lower matching error. The fixed parameter is set to $\rho_0 = 0.6$ and $n = 50$.

References

[1] C. Bregler, A. Hertzmann, and H. Biermann. Recovering non-rigid 3d shape from image streams. *CVPR*, 2000. 1

[2] R. Cabral, F. De la Torre, J. P. Costeira, and A. Bernardino. Unifying nuclear norm and bilinear factorization approaches for low-rank matrix decomposition. *ICCV*, 2013. 4

[3] X. Chen, A. Shrivastava, and A. Gupta. Enriching visual knowledge bases via object discovery and segmentation. *CVPR*, pages 2035–2042, 2014. 1

[4] Y. Chen, L. Guibas, and Q. Huang. Near-optimal joint object matching via convex relaxation. *ICML*, 2014. 1, 2, 3, 4, 5, 8

[5] M. Cho, J. Lee, and K. M. Lee. Reweighted random walks for graph matching. In *ECCV'10*, pages 492–505, 2010. 2

[6] T. Cour, P. Srinivasan, and J. Shi. Balanced graph matching. In *NIPS'06*, pages 313–320, 2006. 1

[7] Y. Dai, H. Li, and M. He. A simple prior-free method for non-rigid structure-from-motion factorization. *CVPR*, 2012. 1

[8] A. Egozi, Y. Keller, and H. Guterman. A probabilistic approach to spectral graph matching. *IEEE Transactions on PAMI*, 99(PrePrints), 2012. 1

[9] D. Emms, R. C. Wilson, and E. R. Hancock. Graph matching using the interference of continuous-time quantum walks. *Pattern Recogn.*, 42(5):985–1002, May 2009. 1

[10] M. Gori, M. Maggini, and L. Sarti. Exact and approximate graph matching using random walks. *IEEE Trans. Pattern Anal. Mach. Intell.*, 27(7):1100–1111, July 2005. 1

[11] T. Hastie, R. Mazumder, L. J, and Z. R. Matrix completion and low-rank svd via fast alternating least squares. *The Journal of Machine Learning Research*, pages 3367–3402, Jan 2015. 4

[12] N. Hu, R. Rustamov, and L. Guibas. Graph matching with anchor nodes: A learning approach. *CVPR*, pages 2906 – 2913, 2013. 1, 2

[13] N. Hu, R. Rustamov, and L. Guibas. Stable and informative spectral signatures for graph matching. *CVPR*, pages 2313 – 2320, 2014. 1, 2, 7

[14] Q.-X. Huang and L. J. Guibas. Consistent shape maps via semidefinite programming. *SGP*, 32(5):177–186, 2013. 1, 2

[15] V. G. Kim, W. Li, N. J. Mitra, S. DiVerdi, and T. A. Funkhouser. Exploring collections of 3d models using fuzzy correspondences. *ACM Trans. Graphics*, 31(4), 2012. 2

[16] D. G. Lowe. Distinctive image features from scale-invariant keypoints. *IJCV*, 60(2):91?110, 2004. 7

[17] K. Mikolajczyk, T. Tuytelaars, C. Schmid, A. Zisserman, J. Matas, F. Schaffalitzky, T. Kadir, and L. Van Gool. A comparison of affine region detectors. *IJCV*, 65(1-2):43?72, 2005. 7

[18] A. Nguyen, M. Ben-Chen, K. Welnicka, Y. Ye, and L. Guibas. An optimization approach to improving collections of shape maps. *Computer Graphics Forum*, 30(5):1481–1491, 2011. 2

[19] D. Pachauri, R. Kondor, and V. Singh. Solving the multi-way matching problem by permutation synchronization. *NIPS*, 2013. 2

[20] B. Recht, M. Fazel, and P. Parrilo. Guaranteed minimum-rank solutions of linear matrix equations via nuclear norm minimization. *SIAM Review*, 52(3):471–501, 2010. 4

[21] S. Umeyama. An eigendecomposition approach to weighted graph matching problems. *IEEE Trans. PAMI*, 10(5):695–703, 1988. 1

[22] A. Vedaldi and B. Fulkerson. *VLFeat: An open and portable library of computer vision algorithms*, 2008. http://www.vlfeat.org/. 7

[23] R. C. Wilson and P. Zhu. A study of graph spectra for comparing graphs and trees. *Pattern Recogn.*, 41(9):2833–2841, Sept. 2008. 1

[24] J. Yan, M. Cho, H. Zha, X. Yang, and S. Chu. Multi-graph matching via affinity optimization with graduated consistency regularization. *IEEE Trans. PAMI*, 2015. 2

[25] C. Zach, M. Klopschitz, and M. Pollefeys. Disambiguating visual relations using loop constraints. In *Computer Vision and Pattern Recognition (CVPR), 2010 IEEE Conference on*, pages 1426–1433, 2010. 2

[26] X. Zhou, M. Zhu, and K. Daniilidis. Multi-image matching via fast alternating minimization. *International Conference on Computer Vision (ICCV)*, 2015. 1, 2, 3, 4, 5, 7, 8

A Proof of Theorem 1

Proof of Theorem 1. Let $G_i - \cdots - G_j - \cdots - G_i$ be a cycle in $\mathcal{G}$. Let $\gamma = \mathcal{V}_i - \cdots - \mathcal{V}_j - \cdots - \mathcal{V}_i$ be the corresponding path in $\mathcal{K}$. W.l.o.g, we assume it is a simple path, i.e. each cover node $\mathcal{V}_j$ appear in p only once except for the starting node $\mathcal{V}_i$. Note assume that any $\mathcal{V}_j$ appears more than once in γ, it could be reduced to appear only once by splitting the cycle into multiple cycles.

$$\mathcal{V}_i - \cdots - \underbrace{\overbrace{\mathcal{V}_j - \cdots - \mathcal{V}_j}}_{\text{first}} - \cdots - \mathcal{V}_i$$

where $\overbrace{\cdot - \cdot}$ means to take the subpath out.

Let's now consider the two cases for γ, 1) $\gamma = \mathcal{V}_i - \mathcal{V}_j - \mathcal{V}_i$, and 2) γ contains more than two cover nodes.

For 1), w.l.o.g., we consider the starting point $G_i \in \mathcal{V}_i \backslash \mathcal{V}_j$ and any $G_j \in \mathcal{V}_j \backslash \mathcal{V}_i$ on the cycle. To show the cycle is consistent is equivalent to show the two composing path γ_1 and γ_2 from G_i to G_j composite to the same map. As shown in Figure 7, if γ_1 and γ_2 share a common vertex (connection point) in $\mathcal{V}_i \cap \mathcal{V}_j$ as in Figure 7(a), then it's easy to see that γ_1 and γ_2 composite to the same map from G_i to G_j by first compositing to the connection point from G_i in $\mathcal{V}_i$ and then to G_j in $\mathcal{V}_j$. If they share different connection points as in Figure 7(b), we could add a cycle path from one connection point to the other in $\mathcal{V}_i \cap \mathcal{V}_j$ ($\mathcal{G}_i$ and $\mathcal{G}_j$ are joint normal) and this reduces to the same as the first case. In addition, $\mathcal{G}_i$ and $\mathcal{G}_j$ being joint normal guarantees there are no edge between G_i and G_j in $\mathcal{G}$ and hence no other cases of possible cycles.

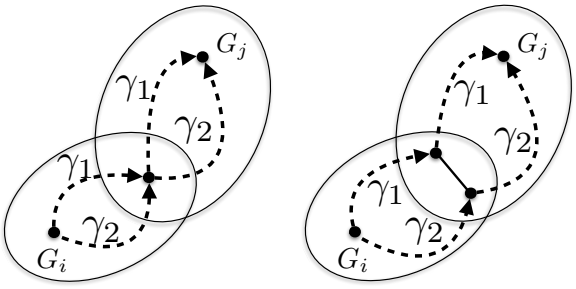

(a) same connection point (b) different connection point

Figure 7: Edge consistency

For 2), since $\mathcal{K}$ is simply connected, we know that it must be the boundary of a subcomplex of $\mathcal{K}$ of dimension 2, or equivalently, is homeomorphic to a disc. To show the cycle is consistent is equivalent to show that for a boundary triangle as show in Figure 8(a) γ_1 and γ_2 are equivalent. That is to say, we could use γ_2 to substitute γ_1 to show cycle consistency of γ_1 and hence remove a boundary triangle.

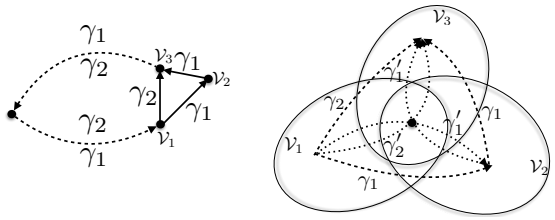

(a) equivalence in triangulation (b) consistency in triangle

Figure 8: Triangle consistency

Recall that the vertices in Figure 8(a) are cover nodes, and Figure 8(b) show an zoom-in of the triangle $\triangle \mathcal{V}_1 \mathcal{V}_2 \mathcal{V}_3$. By adding three consistent cycles, we form two alternating paths γ_1' and γ_2'. It is then easy to see that γ_1 is equivalent to γ_1', equivalent to γ_2', and thus equivalent to γ_2.

By induction, this process of removing one boundary triangle could be kept going on until there is only one triangle left, which reduced to 1), and it's already been proved to be consistent.

□

B Derivation of ADMM Solver

Our final formation of the problem is

$$\begin{array}{ll}\min & \sum_i \left(\langle \mathbf{W}_i, \mathbf{X}_i\rangle + \frac{\lambda}{2}\|\mathbf{A}_i\|_F^2 + \frac{\lambda}{2}\|\mathbf{B}_i\|_F^2\right) \\ \text{s.t.} & \mathbf{X}_i = \mathbf{A}_i\mathbf{B}_i^\top, \\ & \mathbf{E}_{ij}^\top \mathbf{X}_i \mathbf{E}_{ij} = \mathbf{E}_{ji}^\top \mathbf{X}_j \mathbf{E}_{ji}, \\ & \mathbf{X}_i \in \mathcal{C}_i, \end{array} \tag{6}$$

Where $\mathcal{C}_i$ encodes the convex set for the following linear equations,

$$\begin{aligned} \mathbf{X}_{i(jj)} &= \mathbf{I}_{m_j} \\ \mathbf{X}_{i(jk)} &= \mathbf{X}_{i(kj)}^\top \\ 0 \le \mathbf{X}_i &\le 1 \end{aligned}$$

We apply ADMM to (6), and the augmented Lagrangian is

$$\begin{aligned} \mathcal{L} = \sum_i \Bigg(& \langle \mathbf{W}_i, \mathbf{X}_i\rangle + \frac{\lambda}{2}\|\mathbf{A}_i\|_F^2 + \frac{\lambda}{2}\|\mathbf{B}_i\|_F^2 \\ & + \langle \mathbf{Y}_i, \mathbf{X}_i - \mathbf{A}_i\mathbf{B}_i^\top\rangle + \frac{\mu}{2}\|\mathbf{X}_i - \mathbf{A}_i\mathbf{B}_i^\top\|_F^2\Bigg) \\ & + \sum_{i,j} \Big(\langle \mathbf{Z}_{ij}, \mathbf{E}_{ij}^\top \mathbf{X}_i \mathbf{E}_{ij} - \mathbf{E}_{ji}^\top \mathbf{X}_j \mathbf{E}_{ji}\rangle \\ & + \frac{\beta}{2}\|\mathbf{E}_{ij}^\top \mathbf{X}_i \mathbf{E}_{ij} - \mathbf{E}_{ji}^\top \mathbf{X}_j \mathbf{E}_{ji}\|_F^2\Big) \end{aligned} \tag{7}$$

Update on $\mathbf{A}_i$ and $\mathbf{B}_i$ are straightforward and similar, and hence we only show that for $\mathbf{A}_i$. Taking partial derivative of $\mathcal{L}$ over $\mathbf{A}_i$, we have

$$\frac{\partial \mathcal{L}}{\partial \mathbf{A}_i} = \lambda \mathbf{A}_i - \mathbf{Y}_i\mathbf{B}_i - \mu \mathbf{X}_i\mathbf{B}_i + \mu \mathbf{A}_i\mathbf{B}_i^\top\mathbf{B}_i$$

Setting $\frac{\partial \mathcal{L}}{\partial \mathbf{A}_i} = 0$, we have the update on $\mathbf{A}_i$ is

$$\mathbf{A}_i := \left(\mathbf{X}_i + \frac{1}{\mu}\mathbf{Y}_i\right)\mathbf{B}_i\left(\mathbf{B}_i^\top\mathbf{B}_i + \frac{\lambda}{\mu}\mathbf{I}\right)^\dagger$$

Update on $\mathbf{X}_i$ is relatively involved, taking partial derivative of $\mathcal{L}$ over $\mathbf{X}_i$, we have

$$\begin{aligned} \frac{\partial \mathcal{L}}{\partial \mathbf{X}_i} = & \mathbf{W}_i + \mathbf{Y}_i + \mu\mathbf{X}_i - \mu\mathbf{A}_i\mathbf{B}_i^\top \\ & + \sum_j \left(\mathbf{E}_{ij}\mathbf{Z}_{ij}\mathbf{E}_{ij}^\top - \mathbf{E}_{ji}\mathbf{Z}_{ji}\mathbf{E}_{ji}^\top\right) \\ & + 2\beta \sum_j \mathbf{E}_{ij}\left(\mathbf{E}_{ij}^\top \mathbf{X}_i \mathbf{E}_{ij} - \mathbf{E}_{ji}^\top \mathbf{X}_j \mathbf{E}_{ji}\right)\mathbf{E}_{ij}^\top \end{aligned} \tag{8}$$

Therefore, $\mathbf{X}_i$ will be updated to the solution to this linear equation

$$\begin{aligned} \mu\mathbf{X}_i + 2\beta \sum_j \mathbf{E}_{ij}\mathbf{E}_{ij}^\top \mathbf{X}_i \mathbf{E}_{ij}\mathbf{E}_{ij}^\top = & \mu\mathbf{A}_i\mathbf{B}_i^\top - (\mathbf{W}_i + \mathbf{Y}_i) \\ & + \sum_j \mathbf{E}_{ij}\left(2\beta\mathbf{E}_{ji}^\top \mathbf{X}_j \mathbf{E}_{ji} - \mathbf{Z}_{ij} + \mathbf{Z}_{ji}\right)\mathbf{E}_{ij}^\top \end{aligned} \tag{9}$$

LHS of (9) is a linear reweighting on element of $\mathbf{X}_i$. For the $(s,t)^{\text{th}}$ block of $\mathbf{X}_i$, the weight is $\mu + 2\beta d_{st}$, where d_{st} is the degree of replica for e_{st} in the map graph $\mathcal{G}$. While on RHS, $\mathbf{M}_{j\to i} = \mathbf{E}_{ji}^\top \mathbf{X}_j \mathbf{E}_{ji}$ is the message sent from matching graph G_j along e_{ij} in $\mathcal{G}$.

Suppose $\mathbf{X}_{i0}$ is the solution to (9), we need to further project $\mathbf{X}_{i0}$ to $\mathcal{C}_i$, i.e. $\mathcal{P}(\mathbf{X}_{i0})$, which is equivalent to solving the following problem.

$$\begin{array}{ll}\min & \sum_i \|\mathbf{X}_i - \mathbf{X}_{i0}\|_F^2 \\ \text{s.t.} & \mathbf{X}_{i(jj)} = \mathbf{I}_{m_j} \\ & \mathbf{X}_{i(jk)} = \mathbf{X}_{i(kj)}^\top \\ & 0 \le \mathbf{X}_i \le 1 \end{array} \tag{10}$$

This can be easily solved for each block separately,

$$\begin{aligned} \mathbf{X}_{i(jj)} &= \mathbf{I}_{m_j} \\ \mathbf{X}_{i(jk)} &= \min\left(\max\left(\tfrac{1}{2}\left(\mathbf{X}_{i0(jk)} + \mathbf{X}_{i0(kj)}\right), 0\right), 1\right) \end{aligned}$$

where the $\min()$ and $\max()$ is taken element-wise.

The dual update for ADMM is to follow the standard to satisfy the dual feasibility

$$\begin{aligned} \mathbf{Y}_i^{k+1} &\leftarrow \mathbf{Y}_i^k + \mu\left(\mathbf{X}_i - \mathbf{A}_i\mathbf{B}_i^\top\right) \\ \mathbf{Z}_{ij}^{k+1} &\leftarrow \mathbf{Z}_{ij}^k + \beta\left(\mathbf{M}_{i\to j}^{k+1} - \mathbf{M}_{j\to i}^{k+1}\right) \end{aligned}$$